Supplementary Fig. 1 | Study Area Map of the Arabian Peninsula. The seven countries include Bahrain, Kuwait, Oman, Qatar, Saudi Arabia, United Arab Emirates (UAE), Yemen.

Supplementary Fig. 2 | Differential surface warming (°C, left) and population change (millions, right) across all land-cover and land-use change categories in the Arabian Peninsula and seven countries, 2000-2020.

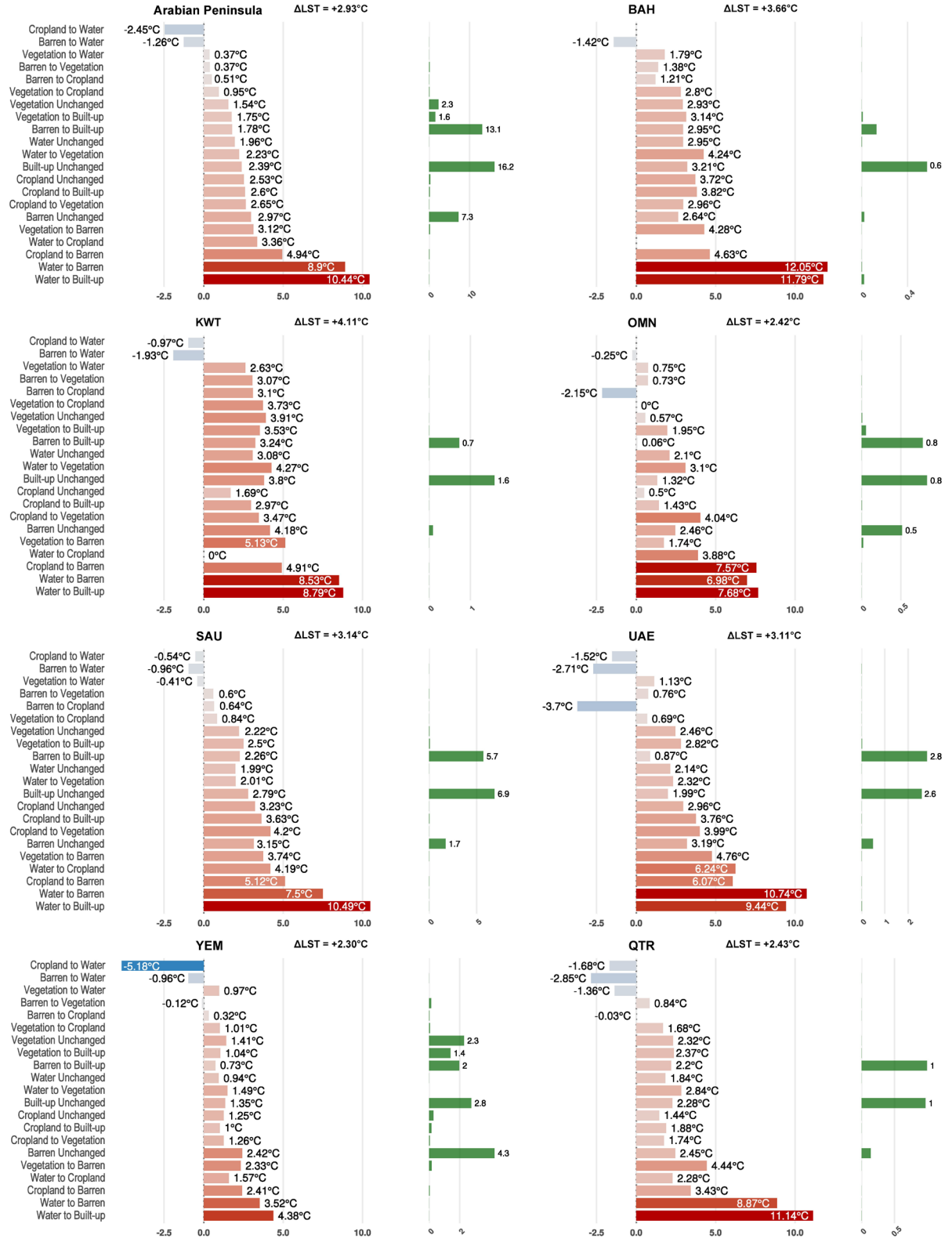

Supplementary Fig. 3 | Spatial patterns of land-cover land-use, population, and land surface temperature in the metropolitan areas of Riyadh, Saudi Arabia and Dubai, the UAE, 2000-2020. a, Patterns of change between 2000-2020 for LCLUC, population change, and LST change (°C). **b,** Regional distributions in 2000 and 2020 showing land cover land use classes, population count at 30m-grid level, and mean annual LST (°C).

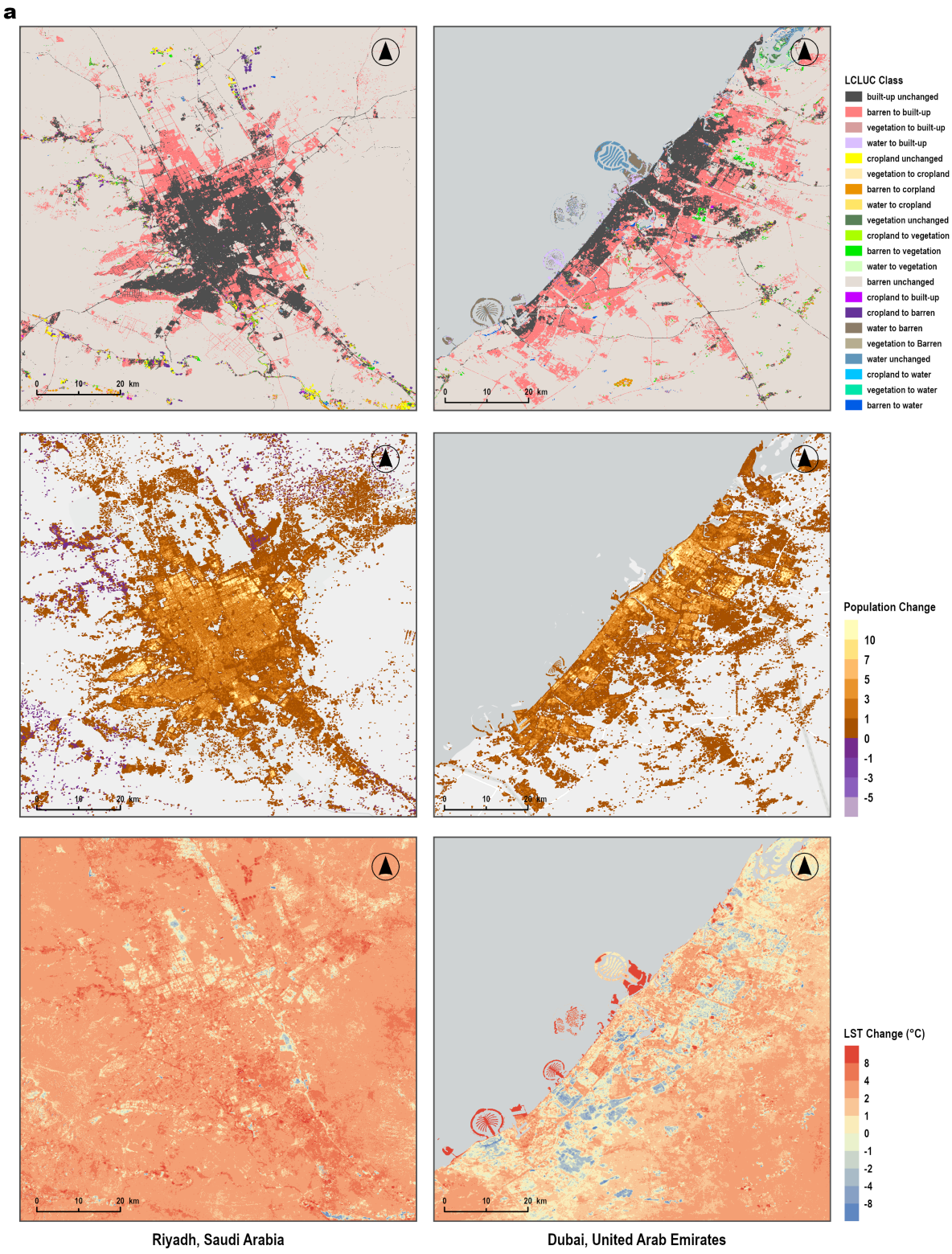

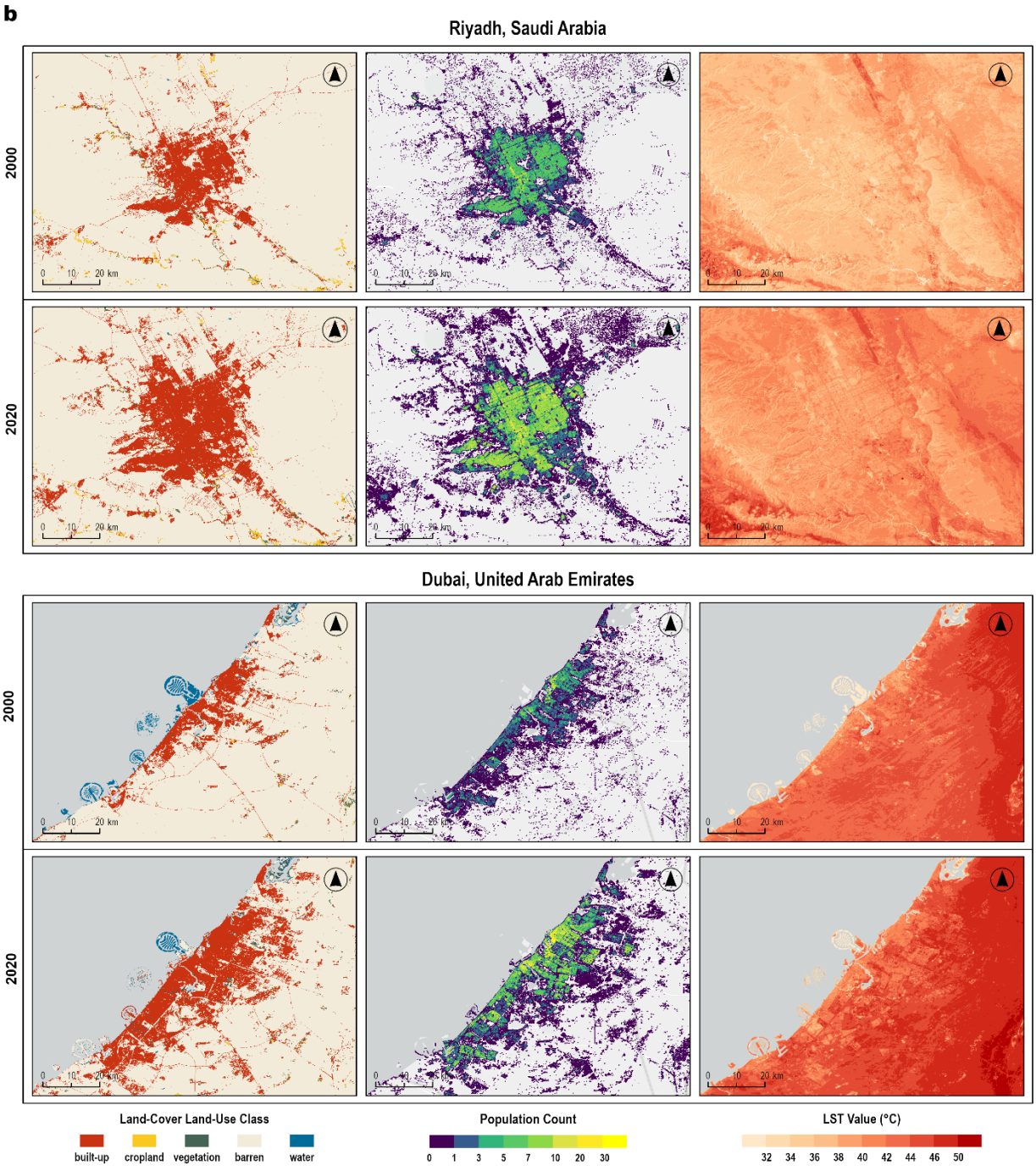
b
Riyadh, Saudi Arabia
2000
2020
Dubai, United Arab Emirates
2000
2020
Land-Cover Land-Use Class
built-up
cropland
vegetation
barren
water
Population Count
0 1 3 5 7 10 20 30
LST Value (°C)
32 34 36 38 40 42 44 46 50

Supplementary Fig. 4 | Spatial comparison of the reclassified land-cover land-use (LCLU) classes between GLAD, Google Dynamic World, ESA World Cover and ESRI Land Cover in selected areas in 2020.

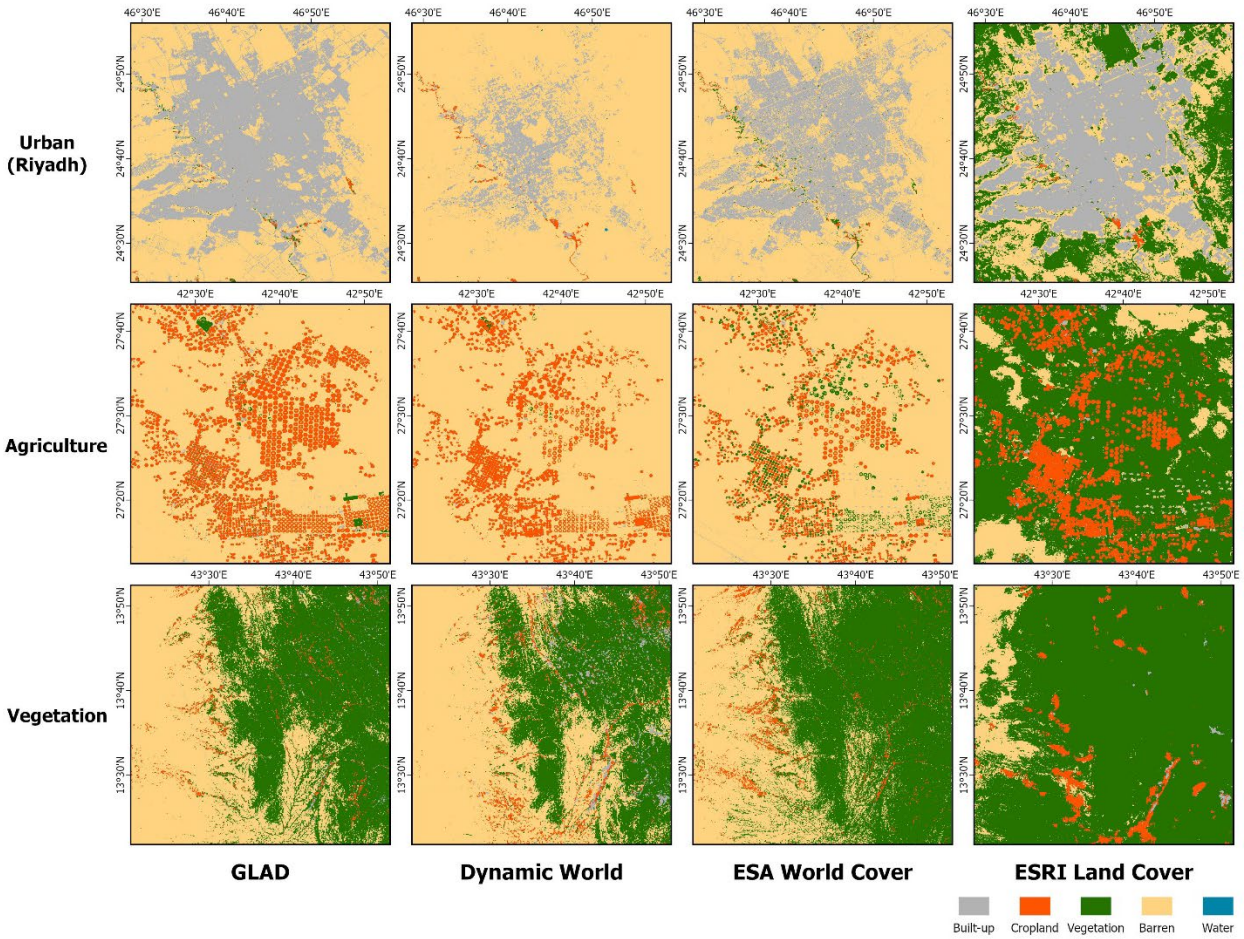

Spatial comparison across three representative regions demonstrates distinct classification patterns between datasets. In the selected urban area (Riyadh), GLAD shows extensive built-up coverage (grey) with scattered barren areas, while Dynamic World and ESA World Cover show more fragmented urban patterns, with less built-up areas. ESRI Land Cover exhibits substantial vegetation overclassification in this arid urban environment. In the agricultural region, all datasets consistently identify the cropland areas (orange), though with varying spatial extents and boundaries. The vegetation region shows the most dramatic differences, with GLAD and ESA World Cover depicting dense vegetation coverage (green), Dynamic World showing mixed vegetation-barren patterns, and ESRI Land Cover displaying widespread vegetation classification extending into traditionally barren areas. Note that cropland overestimation in Dynamic World and ESA World Cover (as shown in Supplementary Table 6) occurs primarily in mountainous and coastal regions not depicted in these selected areas.

Determining the relative accuracy of these datasets remains challenging due to differences in classification schemes, spatial resolution, and temporal coverage. A recent comparative analysis by Venter et al., 2022) evaluated the accuracy of Dynamic World, ESA World Cover, and ESRI Land Cover, finding that accuracy varies significantly by land cover type and geographic region. GLAD was chosen due to its wide range of temporal coverage from 2000-2020.

Supplementary Fig. 5 | An illustration of the annual mean temperature cycle modelled from Landsat-based LST.

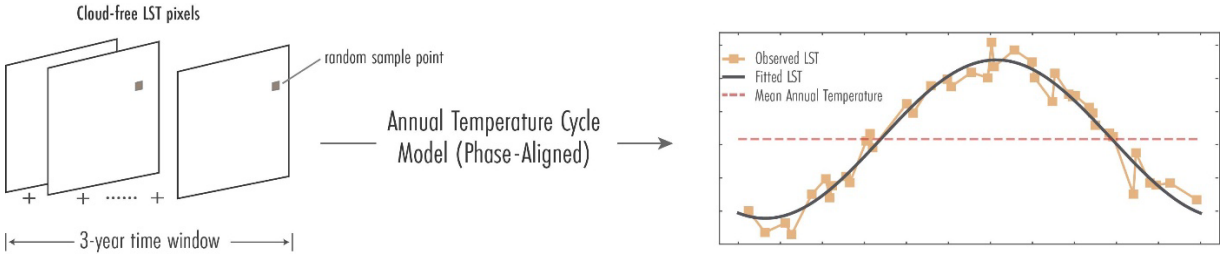

Supplementary Fig. 6 | Comparison of mean annual LST estimates between Landsat and MODIS using harmonic regression: (a) Landsat 2000, (b) MODIS 2000, (c) Landsat 2020 and (d) MODIS 2020.

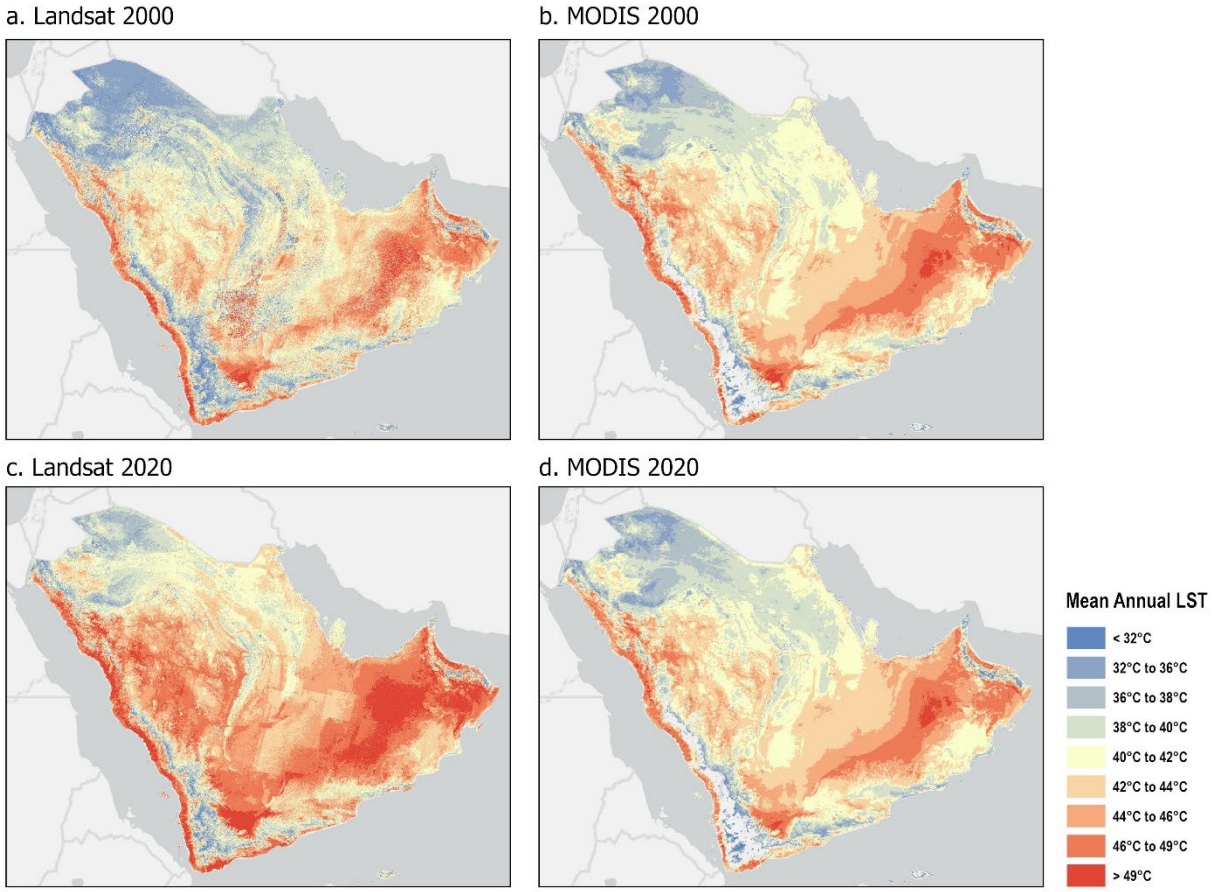

Supplementary Fig. 7 | Spatial distribution of Landsat observation counts and LST model performance across the Arabian Peninsula using a three-year window approach: (a) total observation count 2000, (b) total observation count 2020, (c) root mean square (RMSE) 2000 and (d) RMSE 2020.

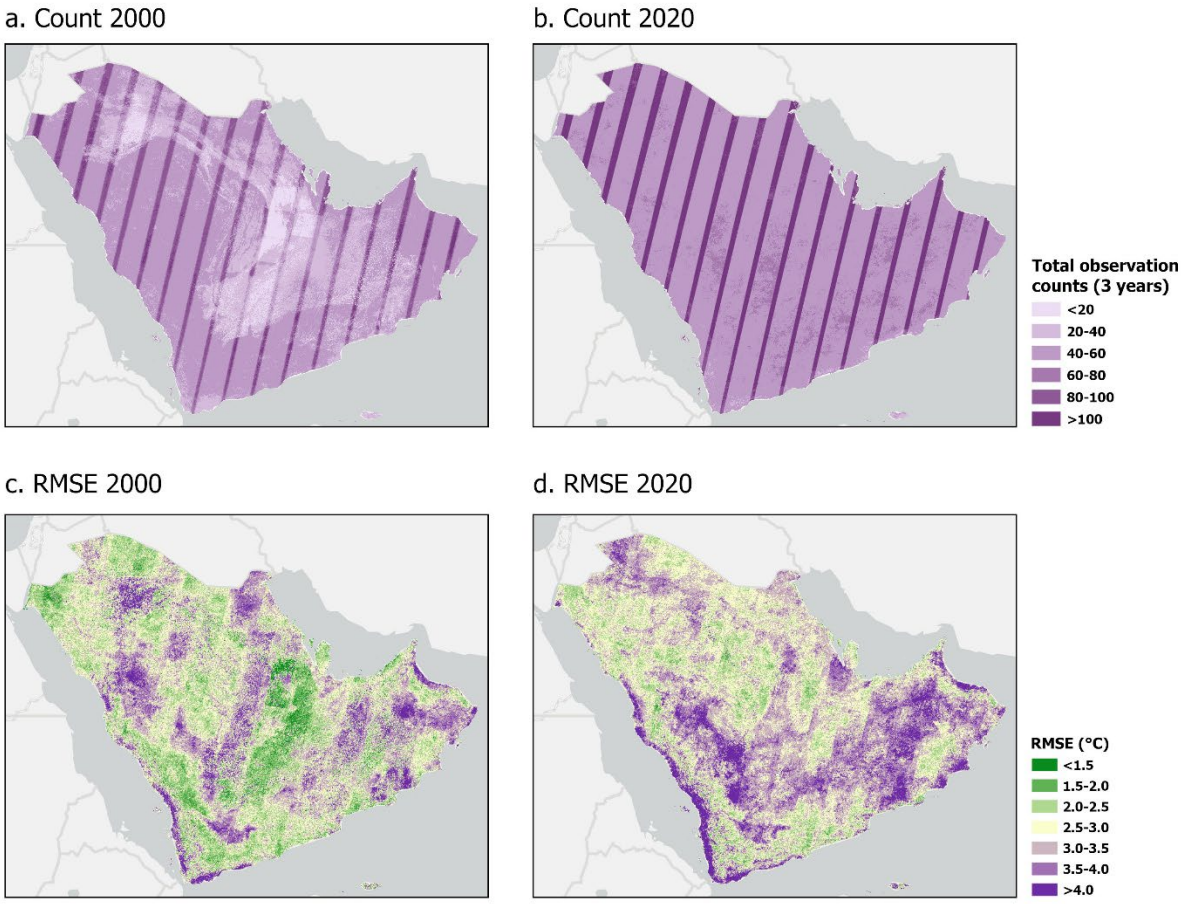

The observation count maps (a, b) reveal the characteristic striped patterns resulting from overlapping Landsat tile boundaries, where pixels receive multiple observations. Coverage improved from 2000 to 2020, with most areas achieving >40 observations over the three-year windows (1999-2001 and 2019-2021). The RMSE maps (c, d) show spatial patterns of harmonic model performance, with lower errors (green areas, <2.5°C) generally occurring in stable desert environments with more consistent thermal properties following simple sinusoidal cycles. Higher RMSE values (purple areas, >3.5°C) indicate areas where the harmonic model has difficulty capturing complex seasonal temperature patterns: (1) coastal areas of the Persian (Arabian) Gulf and Red Sea where land-water thermal contrasts may create complex seasonal patterns, (2) agricultural regions in Saudi Arabia where irrigation cycles introduce seasonal temporal variability, and (3) mountainous areas in Yemen and Oman where topography may affect surface temperature patterns.

Supplementary Fig. 8 | Comparison of Landsat and MODIS LST estimates across LCLU types: (a) 2000, (b) 2020.

(a)

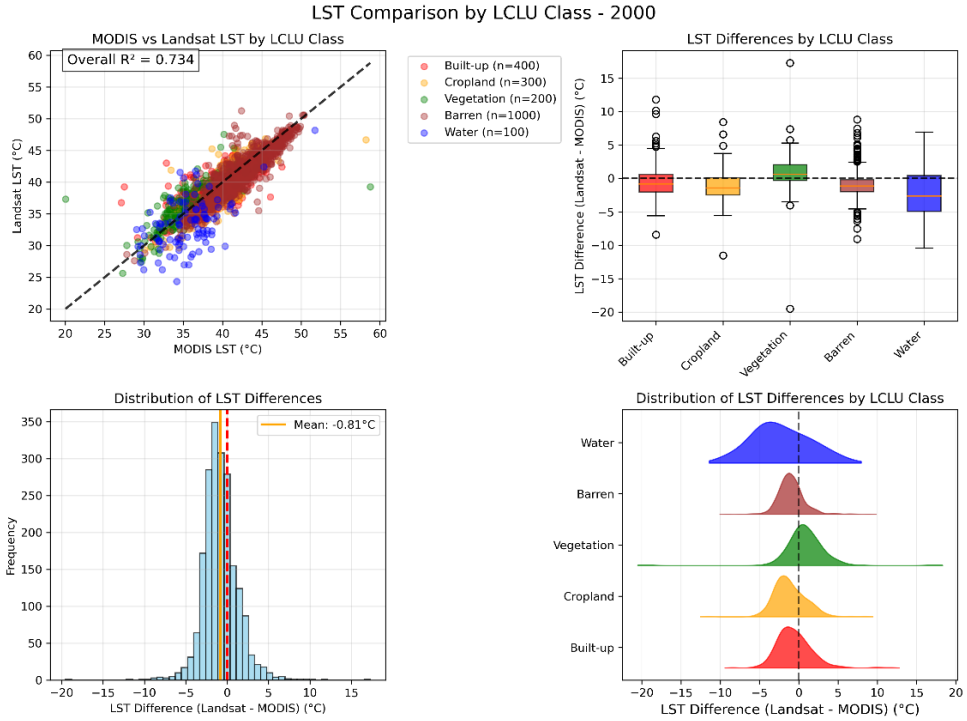

(b)

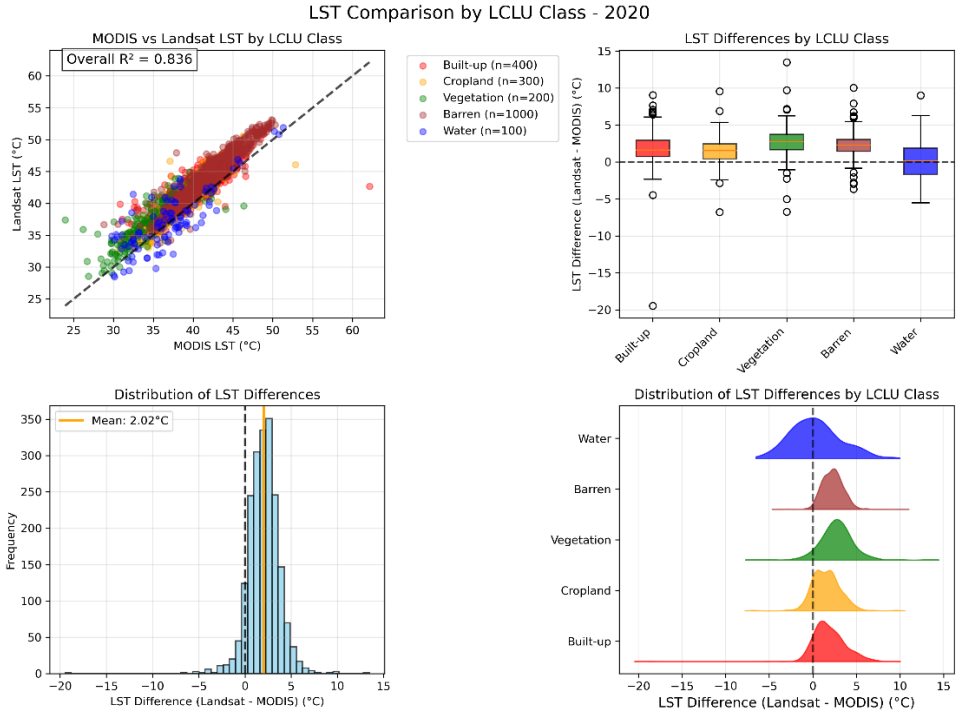

The scatter plots (top-left) demonstrate reasonable linear relationships between Landsat and MODIS LST across both time periods, with most data points clustering around the 1:1 line despite visible scatter. The histogram (bottom-left) shows a shift of the mean LST difference between Landsat and MODIS product from 2000 to 2020, with the distribution patterns remaining relatively stable. The boxplot (top-right) and the ridge plot (bottom-right) distributions show that each land cover type maintains recognizable thermal patterns across both sensors, though with varying degrees of agreement. While systematic differences exist between the two satellite products, the preservation of relative spatial patterns and land cover-specific thermal distributions supports the continued use of Landsat LST for analyzing spatial relationships between land cover change and temperature patterns in this study. However, the observed uncertainties, particularly evident in the 2000 Water class performance and overall scatter, highlight the inherent limitations of satellite-to-satellite inter-comparisons and the importance of considering these uncertainties when interpreting absolute temperature values and temporal changes.

Supplementary Table 1 | Transition matrix of LCLU classes in the Arabian Peninsula 2000-2020. Areas in km^2. See Supplementary Fig. 3 and Table 2 for more LCLUC patterns at country level.

		2020					Total area (2000)
	Class	**Built-up**	**Cropland**	**Vegetation**	**Barren**	**Water**	
2000	**Built-up**	15,274	0	0	0	0	15,274
	Cropland	610	14,911	727	8,146	1	24,395
	Vegetation	2,750	1,196	60,982	4,459	32	69,419
	Barren	17,807	8,213	5,017	3,390,419	1,262	3,422,718
	Water	149	1	38	549	1,401	2,138
	Total area (2020)	36,590	24,321	66,764	3,403,573	2,696	
	Area change (2000-2020)	+21,316	-74	-2,655	-19,145	+558	
	Change rate (2000-2020)	+140.00%	-0.30%	-3.82%	-0.56%	+26.10%	

Supplementary Table 2 | Absolute LCLU changes by countries in the Arabian Peninsula 2000-2020. Areas in km2. All numbers rounded to 0 decimal.

	Built-up				Cropland				Vegetation				Barren				Water			
Country	2000	2020	Change	Rate	2000	2020	Change	Rate	2000	2020	Change	Rate	2000	2020	Change	Rate	2000	2020	Change	Rate
BAH	225	424	199	89%	3	2	-1	-45%	21	6	-14	-70%	616	516	-100	-16%	107	24	-83	-78%
KWT	586	1,362	776	132%	52	77	25	48%	29	41	12	42%	22,568	21,698	-870	-4%	145	202	57	39%
OMN	1,320	3,282	1,963	149%	142	276	134	94%	4,213	3,843	-370	-9%	380,333	378,516	-1816	0%	201	292	90	45%
QTR	377	1,323	946	251%	33	64	31	93%	28	46	18	65%	14,557	13,577	-980	-7%	126	111	-15	-12%
SAU	8,636	20,189	11,553	134%	17,385	16,482	-903	-5%	16,894	16,529	-365	-2%	2,423,719	2,412,996	-10,723	0%	777	1,215	438	56%
UAE	1,857	4,656	2,800	151%	412	106	-306	-74%	494	411	-84	-17%	88,105	85,710	-2,394	-3%	518	503	-15	-3%
YEM	2,276	5,355	3,079	135%	6,368	7,316	948	15%	47,747	45,897	-1,851	-4%	492,968	490,706	-2,262	0%	265	352	86	32%

The magnitude and patterns of LCLUC varied significantly across countries. Besides the rapid expansion of built-up areas, other LCLU classes showed more varying or even contrasting patterns across the region. Regarding cropland, Yemen showed the largest total expansion (+948 km², +15%), while Oman and Qatar achieved remarkable relative increases (+94% and +93%, respectively), despite smaller absolute areas. In contrast, Saudi Arabia experienced substantial cropland losses (-903 km², -5%) and the UAE showed the steepest decline (-306 km², -74%). Regionally, these changes occurred through both new agricultural development (8,213 km² from barren land) and agricultural abandonment (8,146 km² converted to barren), indicating dynamic agricultural transitions across the Arabian Peninsula (Supplementary Table S1. and Supplementary Fig. S4.c). Vegetation patterns were similarly varied, with Yemen experiencing the largest absolute losses (-1,851 km², -4%) and Oman showing significant decreases (-370 km², -9%), while smaller Gulf states like Qatar (+18 km², +65%) and Kuwait (+12 km², +42%) experienced high relative gains. Water bodies increased across most countries, except for Bahrain (-83 km², -78%), Qatar (-15 km², -12%) and UAE (-15 km², -3%).

The sources of urban expansion also differed across the region (Supplementary Fig. S4.c). The vast majority of new built-up areas were converted from barren land, given the predominantly desert landscape. However, some countries showed more diverse conversion pathways. For example, Yemen and Oman have transformed substantial vegetation and cropland areas into built-up areas. Notably, in Bahrain, around 20% of new built-up areas were converted from water bodies through large-scale land reclamation along the Gulf coast (Supplementary Fig. S4.c).

Supplementary Table 3 | Mean land surface temperature and its change by LCLU class in the Arabian Peninsula 2000-2020.

Country	LCLU Class	Mean land surface temperature (°C)		
		2000	2020	ΔLST
Arabian Peninsula	Built-up	38.91	41.81	+2.91
	Cropland	37.88	40.42	+2.54
	Vegetation	36.83	38.4	+1.57
	Barren	41.09	44.06	+2.97
	Water	30.09	34.02	+3.93
	Overall	***40.97***	***43.9***	***+2.93***
Bahrain	Built-up	37.32	40.39	+3.08
	Cropland	36.8	40.38	+3.58
	Vegetation	36.31	38.93	+2.61
	Barren	38.06	40.48	+2.42
	Water	26.61	32.33	+5.72
	Overall	***36.58***	***40.24***	***+3.66***
Kuwait	Built-up	36.39	40.73	+4.35
	Cropland	36.63	39.98	+3.34
	Vegetation	37.12	41.11	+3.99
	Barren	37.8	41.98	+4.18
	Water	25.39	29.13	+3.74
	Overall	***37.68***	***41.79***	***+4.11***
Oman	Built-up	41.39	43.77	+2.39
	Cropland	40.64	42.59	+1.95
	Vegetation	40.4	41.13	+0.72
	Barren	43.45	45.91	+2.45
	Water	30.13	33.46	+3.33
	Overall	***43.41***	***45.83***	***+2.42***
Saudi Arabia	Built-up	38.42	41.91	+3.50
	Cropland	36.31	39.13	+2.81
	Vegetation	35.88	38.22	+2.34
	Barren	40.48	43.63	+3.15
	Water	31.24	35.43	+4.18
	Overall	***40.41***	***43.55***	***+3.14***
United Arab Emirates	Built-up	41.15	43.55	+2.41
	Cropland	40.75	41.18	+0.43
	Vegetation	40.36	42.45	+2.09
	Barren	43.23	46.42	+3.19
	Water	29.2	32.89	+3.7
	Overall	***43.08***	***46.18***	***+3.11***
Yemen	Built-up	38.42	39.43	+1.01
	Cropland	41.92	43.27	+1.36
	Vegetation	36.82	38.2	+1.39
	Barren	42.07	44.49	+2.42
	Water	32.88	34.33	+1.46
	Overall	***41.59***	***43.9***	***+2.3***
Qatar	Built-up	38.21	40.52	+2.32
	Cropland	37.55	38.8	+1.25
	Vegetation	36.39	37.92	+1.53
	Barren	39.05	41.55	+2.5
	Water	28.9	32.48	+3.58
	Overall	***38.94***	***41.37***	***+2.43***

This table reveals a persistent thermal hierarchy across LULC classes in the Arabian Peninsula, where barren lands consistently maintained higher LSTs than built-up areas in both 2000 and 2020. These baseline temperature differences explain why areas converted from barren to built-up maintained higher absolute temperatures than existing urban areas, despite experiencing lower warming rates during urbanization.

Supplementary Table 4 | Resolution sensitivity analysis of bivariate LISA clustering: comparison of cluster composition between 60m analysis (original) and 100m analysis (sensitivity), Arabian Peninsula 2000-2020.

Cluster Type	LCLUC Class	Area (square km)			Composition percentage (%)		
		60m	100m	Difference	60m	100m	Difference (pp)
HH (Growth-Warming)	Built-up unchanged	1340.67	1262.73	-77.94	27.33	26.62	**-0.70**
	Barren to Built-up	986.66	919.26	-67.40	20.11	19.38	**-0.73**
	Barren unchanged	1936.92	1954.67	17.75	39.48	41.21	**1.73**
	Others	641.88	606.26	-35.62	13.08	12.78	**-0.30**
HL (Growth-dominated)	Built-up unchanged	1557.70	1559.64	1.94	19.45	19.79	**0.35**
	Barren to Built-up	3596.23	3829.15	232.92	44.90	48.59	**3.70**
	Barren unchanged	2169.39	1892.74	-276.65	27.08	24.02	**-3.06**
	Others	686.56	598.52	-88.04	8.57	7.60	**-0.98**
LH (Warming-dominated)	Built-up unchanged	1222.75	999.94	-222.81	6.77	8.37	**1.60**
	Barren to Built-up	1022.72	811.61	-211.11	5.66	6.80	**1.13**
	Barren unchanged	12876.42	8192.47	-4683.95	71.29	68.59	**-2.69**
	Others	2940.97	1939.34	-1001.63	16.28	16.24	**-0.04**
LL(Stable)	Built-up unchanged	928.19	672.2	-255.99	7.42	8.10	**0.68**
	Barren to Built-up	1866.54	1568.32	-298.22	14.92	18.90	**3.98**
	Barren unchanged	6890.23	4339.26	-2550.97	55.07	52.30	**-2.77**
	Others	2826.78	1717.14	-1109.64	22.59	20.70	**-1.90**

To assess the robustness of bivariate LISA cluster patterns across different spatial resolutions, we re-ran the bivariate LISA analysis at 100m resolution, which is native to the GHS-based Population grids. LST data were aggregated from 30m to 100m using mean values, LCLUC data were aggregated using modal class. The analysis used identical parameters to the operational 60m analysis, including queen contiguity spatial weights, row standardization, and 999 permutations at $p < 0.05$ significance. We then compared the area and compositional percentage of major LCLUC classes within each cluster type across both resolutions.

The sensitivity analysis demonstrates robust consistency in LCLUC compositional patterns across resolutions, with most percentage point differences under three.

Supplementary Table 5 | Harmonized definition of major LCLU category for the reclassification.

Pixel value	Class	Description
1	Built up	Man-made land surfaces associated with infrastructure, commercial and residential land uses
2	Cropland	Land used to produce annual and perennial herbaceous crops for human activities
3	Vegetation	Land with vegetation cover ≥ 40%
4	Barren	At least 60% of land is non-vegetated barren or permanent snow and ice with < 10% vegetation
5	Water	Ocean or Inland water that covers ≥ 50% of a pixel and is not obscured by objects above the surface

Supplementary Table 6 | LCLU reclassification scheme applied on (**a**) GLAD; (**b**) ESA World Cover; (**c**) Google Dynamic World, and (**d**) ESRI Land Cover datasets.

(**a**)

Original value	Original General class		Original Sub-class	New LULC Class
0	Terra Firma	True desert	3% vegetation cover	Barren
1			7% vegetation cover	
2 – 9		Semi-arid	< 40% vegetation cover	
10 – 18			≥ 40% vegetation cover	Vegetation
19 – 24		Dense short vegetation	≥ 80% vegetation cover	
25 – 48		Stable tree cover	≥ 3m trees	
100	Wetland	Salt pan	3% vegetation cover	Barren
101			7% vegetation cover	
102 – 109		Sparse vegetation	< 40% vegetation cover	
110 – 118			40 – 75 % vegetation cover	Vegetation
119 – 124		Dense short vegetation	≥ 80% vegetation cover	
125 - 148		Stable tree cover	≥ 3m trees	
200	Open surface water		20-29% of year	Water
201			30-39% of year	
202			40-49% of year	
203			50-59% of year	
204			60-69% of year	
205			70-79% of year	
206			80-89% of year	
207			90-100% of year	
241	Snow/ice			Barren
244	Cropland			Cropland
250	Built-up			Built-up
254	Ocean			N/A
255	No data			

(**b**)

Original value	Original Class	New LCLU Class
10	Tree Cover	Vegetation
20	Shrubland	
30	Grassland	
40	Cropland	Cropland
50	Build-up	Build up
60	Bare / sparse vegetation	Barren
70	Snow and Ice	
80	Permanent water bodies	Water
90	Herbaceous wetland	Vegetation
95	Mangroves	
100	Moss and lichen	
0	No data	

(**c**)

Original value	Original Class	New LCLU Class
0	Water bodies	Water
1	Trees	Vegetation
2	Grass	
3	Flooded vegetation	
4	Crops	Cropland
5	Shrub & Scrub	Vegetation
6	Built area	Built up
7	Bare ground	Barren
8	Snow & Ice	
255	No data	

(**d**)

Original value	Original Class	New LCLU Class
1	Water	Water
2	Trees	Vegetation
4	Flooded vegetation	
5	Crops	Cropland
7	Built Area	Built up
8	Bare ground	Barren
9	Snow & Ice	
10	Clouds	No data
11	Rangeland	Vegetation
0	No data	

Supplementary Table 7 | Comparison of LCLU class area estimates (square km) between GLAD and three Sentinel-based datasets in year 2000 for the Arabian Peninsula

LCLU Class	GLAD	ESA World Cover	Difference		Dynamic World	Difference		ESRI Land Cover	Difference	
Built Up	**36,590**	17,099	-19,491	**-53.3%**	15,245	-21,345	**-58.3%**	36,621	31	**+0.1%**
Cropland	**24,321**	35,225	10,904	**+44.8%**	30,717	11,396	**+46.9%**	32,323	8,002	**+32.9%**
Vegetation	**66,765**	93,248	26,483	**+39.7%**	49,241	-17,524	**-26.3%**	1,696,377	1,629,611	**+2441.0%**
Barren	**3,403,574**	3,385,931	-17,643	**-0.5%**	3,430,609	27,035	**+0.8%**	1,764,235	-1,639,339	**-48.1%**
Water	**95,810**	94,785	-1,025	**-1.1%**	96,038	229	**+0.2%**	93,478	-2,331	**-2.4%**

The comparison of GLAD with three Sentinel-based reference datasets reveals notable differences in land cover classification approaches across the Arabian Peninsula. Dynamic World and ESA World Cover underestimate built-up areas by 53-58% compared to GLAD, while ESRI Land Cover shows nearly identical built-up area estimates (+0.1%). Conversely, all three reference datasets identify substantially more cropland areas than GLAD, with differences ranging from +33% to +47%. Visual inspection reveals that Dynamic World's cropland overestimation (+47%) primarily occurs in the Hijaz Mountains range where many vegetated areas are misclassified as agricultural areas, and ESA World Cover's overestimation (+45%) is mostly observed in the Jazan Province in Saudi Arabia. The most pronounced discrepancies are found in vegetation classification, where ESRI Land Cover estimates over 24 times more vegetated area than GLAD (+2,441%), while ESA World Cover shows moderately higher vegetation estimates (+40%) and Dynamic World shows lower values (-26%). Barren land classifications are generally consistent across datasets, except for ESRI which underestimates by 48%. Water body estimates remain relatively consistent across all datasets (±2.4%).

Supplementary Table 8 | Population dataset methodology validation: (a) comparison of population allocation by LCLU class between GHS and Worldpop unconstrained (millions of people) and (b) difference of total population count after resampling from 100m to 30m grid

(a)

Dataset	Year	Built Up	Cropland	Vegetation	Barren	Water	Total	Barren %
GHS-Pop	2000	23.7	5.7	5.9	**18.9**	2.6	49.1	**38.4%**
GHS-Pop	2020	67.7	7.2	6.1	**16.1**	8.5	90.7	**17.8%**
Worldpop	2000	5.6	14.2	8.0	**30.6**	2.3	45.9	**66.7%**
Worldpop	2020	29.3	25.3	12.2	**48.5**	5.2	63.1	**52.1%**

(b)

Dataset	Year	Original 100m	Resampled 30m	Change	% Change
GHS-Pop	2000	49,089,701	49,037,664	-52,037	-0.11%
GHS-Pop	2020	90,713,179	90,708,048	-5,131	-0.01%
Worldpop	2000	45,854,968	45,842,795	-12,173	-0.03%
Worldpop	2020	93,147,984	93,112,020	-35,964	-0.04%

The resampling of population data from 100m to 30m resolution resulted in minimal population loss (<0.11% for all datasets), validating the spatial disaggregation methodology. Population allocation by LCLU class reveals substantial differences between datasets, with WorldPop unconstrained allocating 52-67% of total population to barren desert areas compared to 18-38% for GHS-Pop.

Supplementary Table 9 | Summary statistics of Landsat observation counts and harmonic model performance: (a) the overall summary and (b) mean of metrics by land cover land use type

(a)

Metric	2000	2020
Observation Count		
Mean ± SD	48.2 ± 19.8	66.2 ± 21.9
Median	46	57
% pixels ≥10 observations	71.40%	99.60%
% pixels ≥20 observations	95.10%	100.00%
% pixels ≥40 observations	99.50%	100.00%
RMSE (°C)		
Mean ± SD	2.89 ± 0.72	3.14 ± 0.60
Median	2.83	3.09
25th-75th percentile	2.41 – 3.30	2.73 – 3.49
% pixels <2.5°C RMSE	29.60%	12.30%

(b)

LCLU Class	Mean RMSE 2000 (°C)	Mean RMSE 2020 (°C)	Mean Obs Count 2000	Mean Obs Count 2020
Built-up	2.58 ± 0.57	2.81 ± 0.66	55.8 ± 17.5	64.7 ± 21.3
Cropland	3.65 ± 1.00	3.89 ± 1.05	51.8 ± 15.8	62.5 ± 21.2
Vegetation	2.58 ± 0.63	2.88 ± 0.68	49.5 ± 15.2	56.8 ± 19.3
Barren	2.88 ± 0.80	3.15 ± 0.59	48.1 ± 19.9	66.4 ± 21.9
Water	1.92 ± 0.85	2.30 ±0.97	48.5 ± 16.4	26.9 ± 20.3

Here, the Root Mean Square Error (RMSE) measures the goodness-of-fit between LST observation values and the fitted harmonic model, with higher values indicating stronger temporal patterns that deviate from simple annual cycles. From (a), we can see that data coverage has improved from 2000 to 2020, with mean observation counts increasing from 48.2 to 66.2 per pixel. Yet, the harmonic model performance declined slightly, with the mean RMSE increasing from 2.89°C to 3.14°C. This may result from rapid regional development that created more complex seasonal thermal patterns, and potential sensor-specific differences between Landsat 5 TM (2000) and Landsat 8 TIRS (2020). From (b), we observed that cropland areas showed the highest RMSE values (3.65-3.89°C) due to irrigation-driven temperature seasonality. Water bodies have the lowest RMSE values on average (1.92°C, 2.30°C).

Supplementary Table 10 | Summary statistics of mean annual LST estimate comparison between Landsat-based LST and MODIS daily LST, including coefficient of determination (R^2), root mean square error (RMSE), mean absolute error (MAE), and mean difference (Landsat - MODIS)

LCLU Class	n	2000				2020			
		R^2	RMSE	MAE	Mean Diff.	R^2	RMSE	MAE	Mean Diff.
Overall	2000	0.73	2.32°C	1.78°C	-0.81°C	0.84	2.64°C	2.23°C	+2.03°C
Built-up	400	0.56	2.30°C	1.78°C	-0.58°C	0.65	2.78°C	2.10°C	+1.88°C
Cropland	300	0.65	2.35°C	1.92°C	-1.13°C	0.80	2.24°C	1.75°C	+1.54°C
Vegetation	200	0.60	2.73°C	1.70°C	+0.83°C	0.74	3.38°C	2.90°C	+2.70°C
Barren	1000	0.80	1.91°C	1.52°C	-0.99°C	0.89	2.57°C	2.29°C	+2.26°C
Water	100	0.265	4.31°C	3.61°C	-2.25°C	0.65	2.81°C	2.19°C	+0.33°C

Supplementary Table S7 reveals a strong agreement between Landsat and MODIS LST across both time periods, with coefficients of determination improving from $R^2 = 0.73$ (2000) to $R^2 = 0.84$ (2020). Land cover-specific performance shows consistent patterns, with Barren areas achieving the highest correlation ($R^2 = 0.80$-0.89) and lowest errors, reflecting the thermal homogeneity of desert landscapes. Built-up and Cropland areas demonstrate moderate to good agreement ($R^2 = 0.56$-0.80), while Water bodies show the highest uncertainty but notable improvement over time ($R^2 = 0.265$-0.65), which may be due to uncertainties from the resampling of LCLU layer from 30m to 1km for the stratified sampling. The overall mean difference shifts from -0.81°C to +2.03°C between periods, likely reflecting inherent calibration differences between Landsat 5 TM and Landsat 8 TIRS sensors. Additionally, the comparison methodology itself—extracting MODIS values at point locations versus averaging Landsat values within 1km buffers—may introduce some uncertainty in the absolute differences between the two satellite products. Importantly, this systematic offset affects all land cover types proportionally, suggesting that relative temperature differences and spatial patterns remain reliable for analyzing land cover-temperature relationships.